Thermochimica Acta, 140 (1989) 343–353
Elsevier Science Publishers B.V., Amsterdam – Printed in The Netherlands

THERMAL ANALYSIS OF HETEROCYCLIC THIONE DONOR COMPLEXES. PART VI. PALLADIUM(II) AND PLATINUM(II) COMPLEXES OF THIAZOLE-THIONES

ERIC S. RAPER, AMANDA M. BRITTON and JAMES R. CREIGHTON

Department of Chemical and Life Sciences, The Polytechnic, Newcastle-upon-Tyne NE1 8ST (Gt. Britain)

(Received 31 May 1988)

ABSTRACT

The thermal decomposition of benzothiazoline-2-thione, thiazolidine-2-thione and thiazoline-2-thione complexes of the general formulae $M(LH)_2Cl_2$ and $[M(LH)_4]Cl_2$ ($M = Pd$ and Pt) have been studied in air by means of TG and DTG and by means of DTA in dinitrogen; end-products from the decompositions in air have been characterised by X-ray powder diffraction. Decomposition enthalpies have been determined by quantitative DTA. Decomposition processes have been proposed for the complexes and factors governing thermal decomposition have been discussed.

INTRODUCTION

The thione derivatives of the thiazole molecules used in this study (Fig. 1) are potentially versatile coordinating agents with thioether-S, thione-S and hetero-NH as the major contenders for monodentate donation with divalent

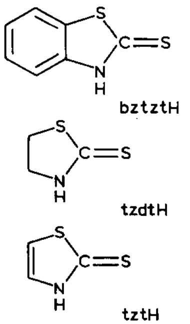

Fig. 1. Molecular formulae and nomenclature.

0040-6031/89/$03.50

metals [1]. Nitrogen donation has been proposed for the Pd(II) and Pt(II) complexes of bztztH and tzdtH on the basis of IR and NMR spectra [2–5]. A single-crystal X-ray study has, however, unequivocally established the monodentate S-donating character of tzdtH in $[Pd(tzdtH)_4]Cl_2$ [6]. No complexes of tztH with Pd(II) and Pt(II) have been previously reported.

This report is concerned with further aspects of the ligating character of tztH, bztztH and tzdtH with Pd(II) and Pt(II) together with the thermal behaviour of the complexes in air and dinitrogen.

EXPERIMENTAL

Materials

All of the ligands were obtained commercially: bztztH as 2-mercaptobenzothiazole and tzdtH as 2-mercaptothiazoline from Ralph N. Emanuel Ltd.; tztH as 2-mercaptothiazole from Lancaster Synthesis. The metal salts, potassium tetrachloroplatinate(II) (K_2PtCl_4) and potassium tetrachloropalladate(II) (K_2PdCl_4), were obtained from The Aldrich Chemical Company Ltd. All reagents were used without further purification.

Preparation and analysis of the complexes

All of the complexes were prepared according to the following general scheme: 1 mmol of K_2MCL_4 M = Pd or Pt) was dissolved in 10 ml of distilled water acidified with 1 M hydrochloric acid. The ligand (stoichiometric amounts were used, 2 or 4 mmol, except in the preparation of $[Pt(tzdtH)_4]Cl_2 \cdot 2H_2O$, where 6 mmol were required) was dissolved in 10 ml of aqueous ethanol, also acidified with 1 M hydrochloric acid. The metal salt solution was then added to the ligand solution, in a dropwise manner, which resulted in immediate precipitation of the relevant complex. The product was filtered, washed with ethanol, dried at 70 °C and stored over $CaCl_2$.

The complexes were characterised by chemical (C, H and N) analyses (Table 1) and IR spectra (4000–200 cm^{-1}), recorded as CsI discs using a Perkin–Elmer 684 IR grating spectrophotometer.

TG and DTG

A Stanton–Redcroft TG 750 thermobalance and DTG unit were used together with open Pt crucibles (6 mm diameter). The atmosphere was column dried (molecular sieve, 13X) in flowing air (20 cm^3 min^{-1}). Sample masses were in the range 2–6 mg, the furnace heating rate was 20 °C min^{-1} and the recorder speed was 5 mm min^{-1}.

DTA

A Stanton–Redcroft 673/4 instrument was used together with quartz crucibles [3 cm (length) and 0.3 cm (internal diameter)]. The latter were chosen in preference to Pt crucibles because of sample swelling and creep as well as the frequent production of tenacious deposits. The furnace atmosphere was flowing dinitrogen (100 cm^3 min^{-1}) and the heating rate was 20 °C min^{-1}. Sample masses were approximately 10 mg, and the reference material was Al_2O_3 (5 mg in a quartz crucible). Amplifier sensitivity was 50 μV (0.5 °C) f.s.d., and the recorder speed was 5 mm min^{-1}. Details of the quantitative DTA method are published elsewhere [7].

X-Ray powder diffraction

A Philips XDC-700 Guinier–Hägg parafocussing camera, monochromatised Cu $K\alpha$ ($\lambda = 154.05$ pm) radiation and single-coated X-ray film were used to identify the end-products in air which were metallic Pt for the Pt complexes (JCPDS reference 4-0802) and metallic Pd or PdO (JCPDS reference 5-0681 (Pd); JCPDS reference 6-0515 (PdO)) for the Pd complexes.

Hot stage microscopy

A Stanton–Redcroft HSM-5 with a Hitachi DK81 video camera and a JVC TM/90 PSN colour monitor were used.

RESULTS AND DISCUSSION

The complexes, together with the stoichiometries, colours and microanalytical data are summarised in Table 1. Data from the TG/DTG curves in air are summarised in Table 2, DTA data in N_2 are summarised in Table 3. Specimen curves are illustrated in Fig. 2 and 3.

Ligands and complexes

The absence of ν(SH), in the region of 2500 cm^{-1}, together with the presence of ν(NH), in the region of 3100 cm^{-1}, as well as the characteristic "thioamide" bands [1] confirmed the presence of the heterocyclic thioamide group, in the ligands, and the dominance of the "thione" tautomeric form in the solid, for both the ligands and their complexes. The monodentate S-donating character of the ligands towards Pd(II) and Pt(II) has been confirmed by the perturbation of the thioamide (IV) bands (800–600 cm^{-1}) and by the detection of ν(M–S) absorptions in the region 310–395 cm^{-1}.

TABLE 1

Analytical data

Compound	(No.)	Colour	RMM	C (%)		H (%)		N (%)		Metal (%) *	
				Found	Calcd.	Found	Calcd.	Found	Calcd.	Found	Calcd.
$[Pt(bztztH)_2Cl_2]$	**(1)**	Yellow	600	29.65	28.0	1.73	1.67	4.75	4.67	32.0	32.5
$[Pt(bztztH)_4]Cl_2 \cdot 2H_2O$	**(2)**	Yellow	970	35.55	34.64	2.21	2.47	5.68	5.77	20.0	20.1
$[Pd(bztztH)_2Cl_2] \cdot H_2O$	**(3)**	Orange	529	33.80	31.76	1.85	2.26	5.35	5.29	19.0	20.0
$[Pd(bztztH)_4]Cl_2$	**(4)**	Dark orange	845	39.60	39.76	2.27	2.37	6.65	6.63	14.5	12.5
$[Pt(tzdtH)_2Cl_2]$	**(5)**	Yellow	504	14.93	14.29	2.00	1.98	5.74	5.56	40.0	38.7
$[Pt(tzdtH)_4]Cl_2 \cdot 2H_2O$	**(6)**	Pale Yellow	778	18.45	18.51	3.00	3.08	7.05	7.20	26.0	25.1
$[Pd(tzdtH)_2Cl_2]$	**(7)**	Orange	415	18.55	17.35	2.45	2.41	7.00	6.75	26.0	25.5
$[Pd(tzdtH)]Cl_2 \cdot 0.5H_2O$	**(8)**	Orange	663	21.63	21.75	3.40	3.17	8.50	8.46	15.5	16.0
$[Pt(tztH)_2Cl_2]$	**(9)**	Yellow	500	14.79	14.40	1.27	1.20	6.01	5.60	40.0	39.0
$[Pt(tztH)_4]Cl_2 \cdot H_2O$	**(10)**	Yellow	752	18.91	19.15	1.85	1.86	7.22	7.45	28.0	26.0
$[Pd(tztH)_2Cl_2]$	**(11)**	Orange	411	20.0	17.52	1.80	1.46	6.79	6.81	28.7	25.8
$[Pd(tztH)_4Cl_2$	**(12)**	Orange	645	22.72	22.32	1.95	1.86	8.93	8.68	16.5	16.5

* % Metal calculated from TG data.

Acidic media were used in the preparation of the complexes in order to inhibit both migration of the labile imido (NH) proton and the de-protonation of the ligands as well as subsequent production of the corresponding thiolato complexes [8,9].

The complexes in this study are characterised by two stoichiometric and structural types. The $[M(LH)_2Cl_2]$ series are neutral species with monoden-

TABLE 2

Thermogravimetric analysis data in air

Compound	(No.)	Overall mass losses			Stepped mass losses	
		Temp. range (° C)	Theo. (%)	Expt. (%)	Temp. Range (° C)	Mass loss (%)
$[Pt(bztztH)_2Cl_2]$	**(1)**	0–475	67.5	68.0	0–310	18
			(Pt)		310–495	50
$[Pt(bztztH)_4]Cl_2 \cdot 2H_2O$	**(2)**	35–475	79.9	80.0	35–169	4
			(Pt)		169–331	44
					331–475	32
$[Pd(bztztH)_2Cl_2] \cdot H_2O$	**(3)**	35–466	76.9	75.0	35–107	3
			(PdO)		107–192	7
					192–370	30
					370–466	35
$[Pd(bztztH)_4]Cl_2$	**(4)**	140–1000	87.5	85.5	140–419	50
			(Pd)		419–466	11
					466–584	18
					584–1000	6.5
$[Pt(tzdtH)_2Cl_2]$	**(5)**	66–628	61.3	60.0	169–399	34
			(Pt)		399–475	26
$[Pt(tzdtH)_4]Cl_2 \cdot 2H_2O$	**(6)**	94–1000	74.9	74.0	94–181	5
			(Pt)		181–409	46
					409–1000	23
$[Pd(tzdtH)_2Cl_2]$	**(7)**	145–539	70.6	70.0	50–230	13
			(PdO)		230–399	31
					399–539	26
$[Pd(tzdtH)_4Cl_2 \cdot 0.5H_2O$	**(8)**	80–521	81.6	82.0	80–169	1.5
			(PdO)		169–370	56.5
					370–521	24
$[Pt(tztH)_2Cl_2]$	**(9)**	51–788	61.0	60.0	51–248	22
			(Pt)		248–788	38
$[Pt(tztH)_4]Cl_2 \cdot H_2O$	**(10)**	94–512	74.0	72.0	94–157	2.5
			(Pt)		157–310	37.5
					310–512	32
$[Pd(tztH)_2Cl_2]$	**(11)**	35–484	70.3	67.0	35–248	9
			(PdO)		248–360	13
					360–484	45
$[Pd(tztH)_4]Cl_2$	**(12)**	66–484	81.1	81.0	66–269	50
			(PdO)		269–484	31

tate S-donating ligands (LH) and are presumed to have *cis*-planar structures on the basis of the reported structure of *cis*-[Pd(tzdtH)$_2$Cl$_2$] [10].

The [M(LH)$_4$]Cl$_2$ series, most of which are hydrated, also contain neutral S-donating ligands with planar [M(LH)$_4$]$^{2+}$ cations and chloride ions. Structural models for this series of complexes include [Pd(tzdtH)$_4$]Cl$_2$ [6] and [M(1-methylimidazoline-2-thione)$_4$]Cl$_2$ · 2H$_2$O (M = Pd and Pt) [11,12]. Both ligands are monodentate S-donating in the above complexes.

Thermogravimetric curves (TG and DTG) in air

*M(LH)$_2$Cl$_2$ series (**1**, **3**, **5**, **7**, **9** and **11**)*

In air the Pd complexes **3**, **7** and **11** thermally degrade to PdO and the Pt complexes **1**, **5** and **9** thermally degrade to the metal. The agreement between theoretical and observed mass losses (Table 2) for the above processes is within experimental error (±2.0%).

The Pd complexes decompose in the temperature range 35–539 °C and a pronounced discontinuity also occurs in the region of 400 °C, at about 40–50% mass loss in each case. Complex **3** is also dehydrated between 35 and 107 °C. The general indication, typified by **7**, is of a two-stage decomposition in which the first stage is somewhat protracted (44% mass loss at 399 °C).

The first stage of decomposition for each of the above is a sequential combination of de-halogenation of the complex followed by de-sulphurisation of the ligands, with concomitant production of the metal sulphide in the residues. Compound **7** shows the clearest indication of these processes among the Pd complexes, with de-halogenation (13% mass loss at 230 °C) and de-sulphurisation of the ligands (44% mass loss at 399 °C) followed by conversion into the oxide (70% mass loss at 539 °C). The two components of the first stage were indicated by clear separation on their DTG curves. Among the Pt complexes the discontinuity (34% mass loss at 399 °C) in **5** also represents a combination of de-halogenation and de-sulphurisation, followed by conversion of the sulphide residue to the metal (60% mass loss at 475 °C).

*M(LH)$_4$Cl$_2$ series (**2**, **4**, **6**, **8**, **10** and **12**)*

The Pt complexes **2**, **6** and **10** as well as [Pd(tzdtH)$_4$]Cl$_2$ · 0.5H$_2$O **8** are hydrated. Thermal decomposition to the metal in air occurs with the Pt complexes together with [Pd(bztztH)$_4$]Cl$_2$ **4**. The remaining Pd complexes **8**, **12** thermally degrade to PdO. Agreement between theoretical and observed mass losses for the above processes is within experimental error (±2.0%).

The hydrated complexes **2**, **6**, **8** and **10** smoothly dehydrate at temperatures which extend up to 191 °C in one instance (**6**). Dehydration is invariably indicated by a single stage on both TG and DTG curves. Thermal decomposition of the complexes is generally completed at about 800 °C with

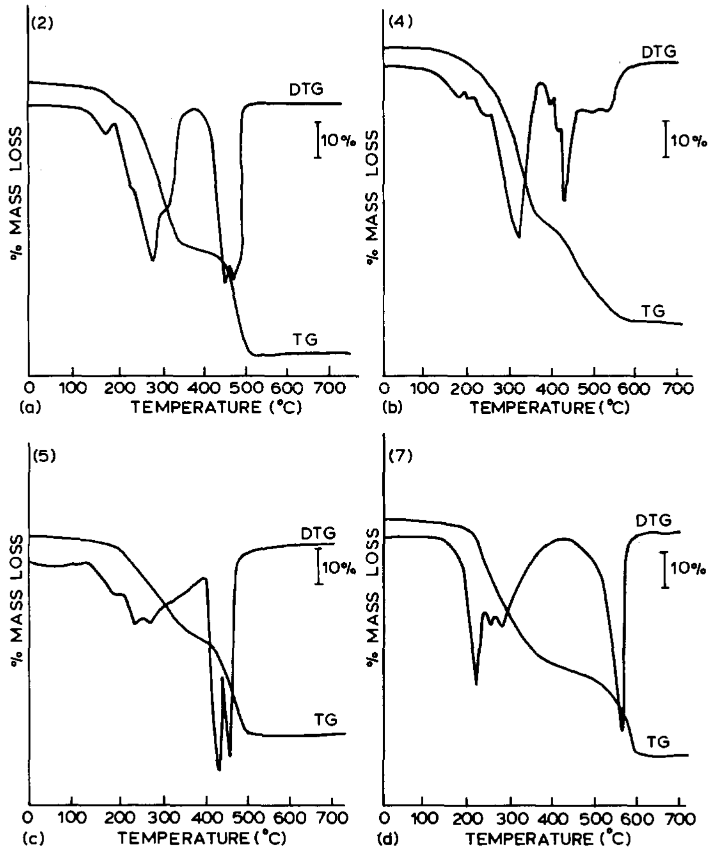

Fig. 2. TG and DTG curves for (a) $[Pt(bztztH)_4]Cl_2 \cdot 2H_2O$, (b) $[Pd(bztztH)_4]Cl_2$, (c) $[Pt(tzdtH)_2Cl_2]$ and (d) $[Pd(tzdtH)_2Cl_2]$.

the exception of **4** and **6**; in these cases, the decomposition temperature extends to 1000 °C.

The Pd complexes all show a substantial, initial mass loss (44–50%) followed by a somewhat smaller mass loss (24–35%). The Pt complexes similarly decompose in essentially two stages, again with the first mass loss (38–46%) somewhat larger than the second (23–33%).

The first mass loss, for the above complexes, involves desulphurisation of the ligands with concomitant metal sulphide production. The second stage involves decomposition of the residual metal sulphides and chlorides to the metal (**2**, **4**, **6** and **10**) or PdO (**8** and **12**). Among the Pd complexes **4** clearly shows complete de-sulphurisation of the ligands (50% mass loss at 419 °C) followed by a sharp mass loss (61% at 466 °C) which is attributed to de-halogenation. The final two stages involve conversion of the sulphide to the oxide (79% mass loss at 584 °C) and oxide to the metal (85.5% mass loss at 1000 °C) together with progressive oxidation of carbonised residues resulting from the de-sulphurisation stage.

Among the Pt complexes **2** is completely de-sulphurised in a single stage (TG) although the DTG peak has three clearly indicated components (48% mass loss at 331 °C). The final stage (80% mass loss at 475 °C) is characterised by two contiguous components in the DTG curve and involves a combination of de-halogenation and conversion of the metal sulphide to the metal.

DTA curves in N_2

Ligands

Each of the ligands shows two sharp endotherms, involving melting (69–226 °C) and decomposition (226–399 °C). The overall sublimation enthalpies for bztztH, tzdtH and tztH are 96.5, 65.8 and 68.7 kJ mol^{-1} respectively.

$M(LH)_2Cl_2$ series

The Pd complexes **3**, **7** and **11** decompose in the temperature range 107–309 °C. Compounds **3** and **11** exhibit two distinct endotherms, whereas **7** shows three endotherms. Overall decomposition enthalpies range from 63.9 (**11**) to 110.6 kJ mol^{-1} (**3**).

The Pt complexes **1**, **5** and **9** show either two (**1**) or three endotherms (**5** and **9**) in the temperature range 130–503 °C. Overall decomposition enthalpies range from 111.8 (**5**) to 130.8 kJ mol^{-1} (**9**). Endotherms tend to be broad rather than sharp in character and hot stage microscopy revealed that no distinctive melting occurred for any of the above complexes. The temperature range of the decompositions in N_2 broadly parallels the thermal events shown by the TG and DTG curves in air, which correspond to de-halogenation and de-sulphurisation of the complexes.

The sublimation enthalpies of the ligands indicate that the minimum energy requirements for the ligand evolution should range from 131.6 (tzdtH) to 193.0 kJ mol^{-1} (bztztH). If we add to these values the energy requirements for metal–ligand dissociation (120–150 kJ mol^{-1}) [7] and the metal halide dissociation (200–300 kJ mol^{-1}) [13], then the total energy requirements for sequential loss of ligand and halide from the complexes can be seen to be considerably greater than the enthalpies derived from the DTA curves. Consequently, the decomposition enthalpies of the complexes are indicative of a combination of thermal events involving endothermic ligand de-sulphurisation and de-halogenation and exothermic metal sulphide formation.

$M(LH)_4Cl_2$ series (2, 4, 6, 8, 10 and 12)

The Pd complexes **4**, **8** and **12** show either three (**4** and **8**) or four endotherms (**12**), in the temperature range 94–399 °C. Total decomposition enthalpies are in the range 248.0 (**8**) to 282.1 kJ mol^{-1} (**12**).

TABLE 3

Differential thermal analysis data in dinitrogen

Compound	(No.)	DTA peak (T_m/° C)	Peak range (T/° C)	Enthalpy (ΔH_R/kJ mol^{-1})
bztztH		192	157–226	40.8 (±1.7)
		360	360–399	55.7 (±0.2)
[Pt(bztztH)$_2$Cl$_2$]	**(1)**	222	187–258	87.8 (±5.5)
		471	428–503	36.1 (±0.2)
[Pt(bztztH)$_4$]Cl$_2$·2H$_2$O	**(2)**	215	157–243	48.1 (±2.1)
		279	254–300	100.0 (±7.7)
		350	310–390	76.6 *
[Pd(bztztH)$_2$Cl$_2$]·H$_2$O	**(3)**	204	107–269	65.9 (±12.9)
		350	310–390	44.7 (±3.8)
[Pd(bztztH)$_4$]Cl$_2$	**(4)**	210	107–237	57.7 (±2.0)
		282	248–320	164.0 (±18.5)
		360	346–399	37.9 (±6.3)
tzdtH		107	80–133	19.9 (±0.7)
		290	226–331	45.9 (±3.6)
[Pt(tzdtH)$_2$Cl$_2$]	**(5)**	140	130–152	9.3 (±0.1)
		184	169–199	13.5 (±0.5)
		254	223–310	89.0 (±7.4)
[Pt(tztdH)$_4$]Cl$_2$·2H$_2$O	**(6)**	140	120–157	104.3 (±1.1)
		254	210–290	170.5 (±5.4)
		315	290–341	20.0 (±0.1)
[Pd(tzdtH)$_2$Cl$_2$]	**(7)**	157	145–204	21.8 (±0.4)
		232	204–290	50.9 (±0.5)
		310	290–346	7.3 (±0.8)
[Pd(tzdtH)$_4$]Cl$_2$	**(8)**	100	94–145	45.2 (±1.0)
		232	204–290	154.1 (±1.3)
		318	302–380	48.7 (±6.2)
tztH		80	69–107	33.9 (±3.0)
		300	232–336	34.8 (±0.9)
[Pt(tztH)$_2$Cl$_2$]	**(9)**	157	131–169	4.2 (±0.2)
		237	215–248	1.8 (±0.1)
		290	248–362	124.8 (±2.2)
[Pt(tztH)$_4$]Cl$_2$	**(10)**	133	87–163	77.1 (±2.5)
		258	204–291	143.3 (±2.0)
		300	291–320	20.8 (±2.2)
[Pd(tztH)$_2$Cl$_2$]	**(11)**	192	163–226	12.9 (±1.4)
		269	254–350	51.0 (±0.6)
[Pd(tztH)$_4$]Cl$_2$	**(12)**	114	94–145	6.0 (±0.2)
		243	192–258	116.2 (±7.5)
		269	258–290	86.4 (±2.4)
		310	290–331	73.5 (±1.8)

* Irreproducible.

The Pt complexes **2**, **6** and **10** thermally degrade in the temperature range 87–390 °C and all of the complexes exhibit three endotherms with overall decomposition enthalpies in the range 224.7 (**2**) to 294.6 kJ mol^{-1} (**6**). No

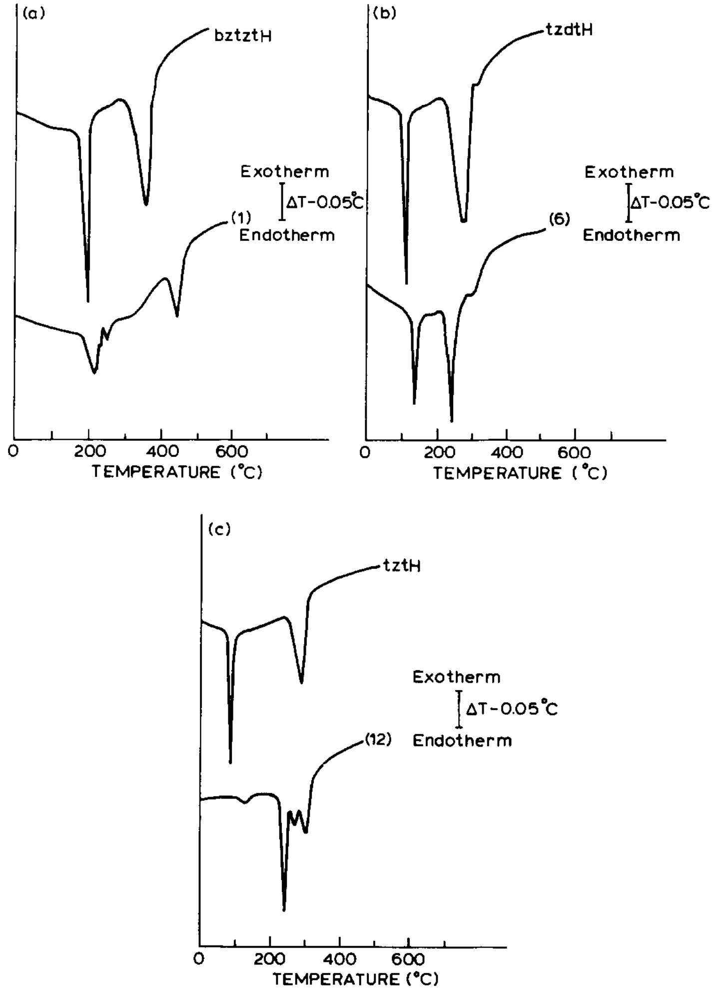

Fig. 3. DTA curves in dinitrogen for (a) bztztH and $[Pt(bztztH)_2Cl_2]$, (b) tzdtH and $[Pt(tzdtH)_4]Cl_2 \cdot 2H_2O$ and (c) tztH and $[Pd(tztH)_4]Cl_2$.

distinctive dehydration or melting endotherms were observed for the above complexes, either from the individual curves or by means of hot stage microscopy. All DTA curves were broad rather than sharp and the temperature range of the decompositions broadly parallels the de-sulphurisation and de-halogenation processes observed from the TG and DTG curves in air.

Consideration of the decomposition enthalpies, deduced from the DTA curves, again suggests that decomposition of the complexes involves a combination of endothermic ligand de-sulphurisation and decomposition coupled with endothermic de-halogenation and exothermic metal sulphide formation. The alternative processes of ligand evolution involve significantly greater endothermic requirements, e.g. 386 (bztztH) and 263.2 kJ mol^{-1} (tzdtH) for ligand sublimation alone.

Final Comments

The presence of Pd–S and Pt–S bonds in the complexes, as well as that of heterocyclic sulphur in the ligands, determines that the ligands decompose, rather than evolve unchanged, during thermal decomposition. Metal–sulphur links are retained and extended, owing to metal sulphide formation, during thermal decomposition. These factors explain the presence of discontinuities and the absence of plateaux on the TG curves since all intermediates are precursors in the production of the metals or PdO. Similar behaviour has been reported for the dithiooxamide complexes of Pd and Pt [14].

The nature of the chloride is an interesting conditioner of thermal behaviour. Coordinated chloride is slowly and initially evolved whereas ionic chloride is retained until the final stages of thermal decomposition. Chemical tests on the evolved gases support these observations.

REFERENCES

1 E.S. Raper, Coord. Chem. Rev, 61 (1985) 115.
2 J. Dehand and J. Jordanov, Inorg. Chim. Acta, 17 (1976) 37.
3 R.F. Wilson and P. Merchant, J. Inorg. Nucl. Chem., 29 (1967) 1993.
4 D. DeFilippo, F. Devillanova, E.F. Trogu, C. Preti and P. Viglino, Can. J. Chem., 51 (1973) 1172.
5 G. Colombini and C. Preti, J. Inorg. Nucl. Chem., 87 (1975) 1159.
6 M. Kubiak and T. Glowiak, Acta Crystallogr., Sect. B, 38 (1982) 2031.
7 E.S. Raper, J. Therm. Anal., 25 (1982) 463.
8 M. Kubiak, Acta Crystallogr., Sect. C, 41 (1985) 1288.
9 E.S. Raper, A.M. Britton, J.R. Creighton, W. Clegg, M. Hooper and M. Kubiak, Acta Crystallogr., Sect. C, 43 (1987) 1538.
10 M. Kubiak, Proc. School Symposium in Inorganic Biochemistry and Molecular Biophysics, Institute of Chemistry, University of Wroclaw, Karpacz, Poland, 1985, p. 178.
11 M. O'Neill, E.S. Raper, J.A. Daniels and I.W. Nowell, Inorg. Chim. Acta, 66 (1982) 79.
12 L.M. Butler, J.R. Creighton, R.E. Oughtred, E.S. Raper and I.W. Nowell, Inorg. Chim. Acta, 75 (1983) 149.
13 M.C. Ball and A.H. Norbury, Physical Data for Inorganic Chemists, Longman, 1974, p. 78.
14 H. Hofman and H.O. Desseyn, Thermochim. Acta, 85 (1985) 67.